Both VP2 and VP3 Are Synthesized from Each of the Alternatively Spliced Late 19S RNA Species of Simian Virus 40

PETER J. GOOD, RENÉE C. WELCH, ALICE BARKAN,† MADHU B. SOMASEKHAR,‡ AND JANET E. MERTZ*

McArdle Laboratory for Cancer Research, University of Wisconsin, Madison, Wisconsin 53706

The late 19S RNAs of simian virus 40 consist of a family of alternatively spliced RNAs, each of which contains open reading frames corresponding to all three of the virion proteins. Two approaches were used to test the hypothesis that each alternatively spliced 19S RNA species is translated to synthesize preferentially only one of the virion proteins. First, we analyzed the synthesis of virion proteins in simian virus 40 mutant-infected monkey cells that accumulate predominantly either only one spliced 19S RNA species or only the 19S RNAs. Second, we determined the virion proteins synthesized in a rabbit reticulocyte lysate programmed with specific, in vitro-transcribed 19S RNA species. These results indicated that VP2 and VP3, but not VP1, are synthesized from all 19S RNA species. Quantitative analysis of these data indicated that individual 19S RNA species containing a translation initiation signal upstream of the VP2 AUG codon were translated in a cell extract three- to fivefold less efficiently than were 19S RNA species lacking this signal and that the precise rate of synthesis of VP2 relative to VP3 varied somewhat with the sequence of the leader region. These data are consistent with the synthesis of VP2 and VP3 occurring by a leaky scanning mechanism in which initiation of translation at a specific AUG codon is affected by both (i) the intrinsic efficiency of ribosomes recognizing the sequences surrounding the AUG codon as an initiation signal and (ii) partial interference from 5'-proximal initiation signals and their corresponding open reading frames.

The papovaviruses are double-stranded DNA viruses whose genome sizes are severely limited by packaging constraints. These viruses overcome their size limitations by several mechanisms which increase the overall coding capacities of their genomes. In simian virus 40 (SV40), alternative RNA processing generates multiple late RNA species and the translation of overlapping open reading frames (ORFs) results in the synthesis of four late proteins (32, 57). We were interested in knowing whether each of the alternatively spliced RNA species is preferentially translated to synthesize only one of the virion proteins.

Cells infected with SV40 accumulate two classes of late RNAs, 16S and 19S in size (see reference 57 for a review and Fig. 1 for structures). All of the spliced 19S RNAs are processed by using a 3' splice site at nucleotide residue (nt) 558 and one of three 5' splice sites (15); RNA species F is a doubly spliced RNA species (18). All of the 16S RNAs lack an intervening sequence (intron) mapping from nt 527 through nt 1462, with minor RNA species lacking additional introns encoded within the leader region (47).

Each of the late 19S RNA species contains the ORFs for all three of the virion proteins, VP1, VP2, and VP3; RNA species E encodes LP1 (also called agnoprotein) as well (57). VP2 and VP3 are encoded within the same reading frame, with the amino acid sequence of VP3 corresponding to the carboxy-terminal two-thirds of VP2 (10). Nevertheless, VP3 is synthesized independently of VP2, starting from its own translation initiation codon at nt 916, instead of by proteolytic processing of VP2 (8, 9, 50, 51). Translation of VP2 and VP3 terminates 119 nt downstream of the initiation codon used in the synthesis of VP1 (Fig. 1). The 16S RNA species

lack an intron that encodes the amino terminus of VP2 and VP3; they therefore encode only VP1 and LP1 or, for RNA species H, only VP1 (7, 47).

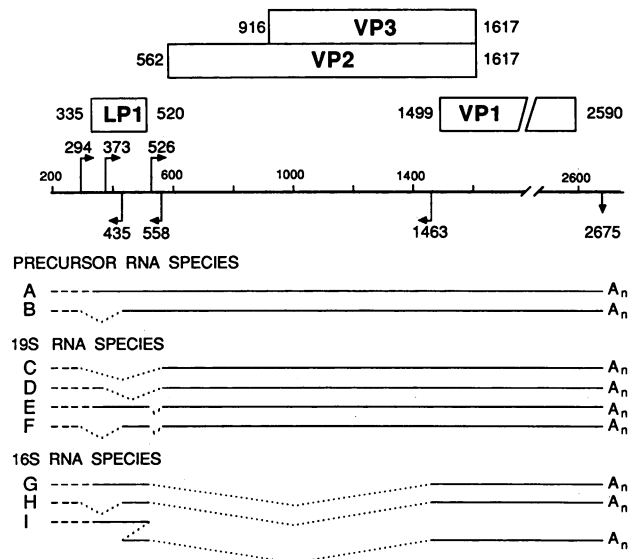The existence of multiple 19S RNAs differing only in the

FIG. 1. Map of the late region of SV40. The numbered line represents SV40 DNA with the nucleotide residue numbers being in the SV numbering system (57). The rightward and leftward arrows indicate the locations of 5' and 3' splice sites, respectively. The downward arrow indicates the site of cleavage and polyadenylation. The lines below the DNA show the structures of the late RNAs: . . . . ., locations of excised intervening sequences; – – – –, heterogeneity in the locations of the 5' ends (15, 54). The boxes above the DNA indicate the proteins encoded within the late region; the numbers adjacent to them indicate the first and last nucleotides translated.

* Corresponding author.
† Present address: Department of Genetics, University of California Berkeley, Berkeley, CA 94720.
‡ Present address: Department of Physiology and Biophysics, University of Iowa, Iowa City, IA 52242.

precise sequence of their leader regions has led to the proposal that each 19S RNA species is translated to synthesize preferentially only one of the virion proteins (1, 35). Thus, the rates of synthesis of the late proteins would be regulated by the amounts of the different spliced 19S RNA species. For example, polyomavirus, a papovavirus with a genomic organization similar to that of SV40, is known to synthesize spliced late RNA species specific for each virion protein (22, 53). Hypotheses to explain how the sequence of the leader might affect translation of the downstream ORFs include the following. (i) The sequence immediately upstream of the VP2 initiation codon, determined by the 5' splice site used in processing of the primary transcript, influences the efficiency of utilization of this initiation signal. (ii) By determining the secondary structure of the RNA, the precise sequence of the leader region influences the ability of the translation machinery to recognize specific initiation signals (31). (iii) Translation of upstream ORFs, which differs for the different spliced 19S RNA species, affects in cis the translation of the downstream ORFs. (iv) The proteins encoded within the leader regions affect differentially and in trans the translation of the various RNA species (1).

We have tested whether each of the alternatively spliced 19S RNA species is translated to synthesize preferentially only one of the virion proteins. Analysis of the virion proteins synthesized in cells that accumulate the late RNA species in altered ratios and in rabbit reticulocyte lysates programmed with each of the specific spliced 19S RNA species showed that both VP2 and VP3, but not VP1, are synthesized from each of the 19S RNA species. The overall efficiency of translation and rate of synthesis of VP2 relative to VP3 varied among the specific RNA species. Therefore, in agreement with a leaky scanning model for translation initiation, the relative strengths of the translation initiation signals, together with effects of translation of upstream ORFs on the translation of downstream ones, determine the rates of synthesis of the virion proteins from each of the late 19S RNA species.

MATERIALS AND METHODS

Cells and viruses. MA-134, CV-1P, and CV-1PD (obtained from C. Cole) are established lines of African green monkey kidney cells. The origin, growth characteristics, and biological properties of the wild-type (WT) SV40 strain WT800 and mutants 802, 805, 806, and 809 have been reported previously (4). Mutant 810-R3 was isolated by plaque purification from a serially passaged virus stock of mutant 810 (4) and contains a 26-base-pair duplication of the leader region from nt 483 through nt 508, inclusive (M. B. Somasekhar, A. Barkan, K. Cohen, and J. E. Mertz, manuscript in preparation). Virus stocks were prepared from plaque-purified virus, and their titers were determined as described previously (38). Strain WT830 and mutant 1770 viruses were generated, respectively, from pSVS and pSV1770 by excision of the viral genomes from the vector sequences, ligation into monomer circles, and transfection into CV-1P cells. Complementation tests were performed as described previously (38); however, in place of temperature-sensitive mutants as standards, we used nonviable mutants that had been propagated as plasmids in bacteria, excised from the cloning vector, and ligated into monomer circles prior to use. Mutants SV1773 and SV1774 served as standards for the B and D complementation groups, respectively.

Plasmids. Recombinant DNAs were manipulated as described previously (36). Restriction and modifying enzymes
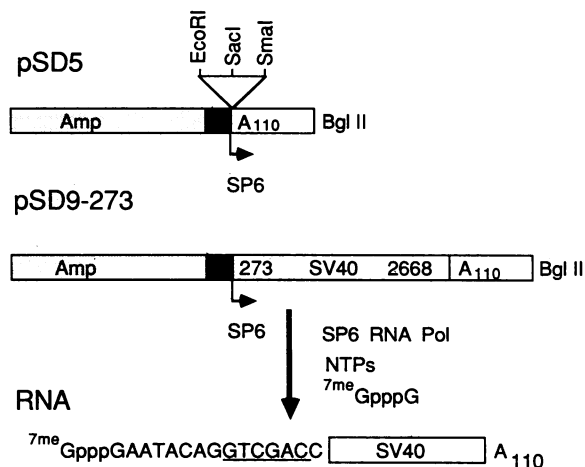

FIG. 2. Structures of BglII-linearized SP6 promoter vectors and the transcript made from pSD9-273. For plasmid pSD5: ▭, pSP65 sequences; ■, SP6 promoter; ▭, stretch of approximately 110 poly(dA) residues encoded within the DNA. The triangle above the SP6 promoter indicates the restriction sites remaining from the pSP65 polylinker. Plasmid pSD9-273 has the SV40 late region from nt 273 through nt 2668, indicated by the box labeled SV40, inserted between the EcoRI and SmaI sites of pSD5. The sequence of the transcript synthesized from pSD9-273 by SP6 RNA polymerase in the presence of ^{7me}GpppG is indicated at the bottom. The SalI site used in the insertion of restriction fragments from the late 19S cDNAs is underlined.

and linker DNAs were purchased from New England Bio-Labs, Inc., Promega Biotec, and Boehringer Mannheim Biochemicals and used interchangeably. The exact structure of each plasmid was confirmed by restriction enzyme digestion and, when necessary, nucleotide sequence analysis. All nucleotide numbers refer to the SV numbering system (57). Plasmid pSV1770 was constructed by cleavage of plasmid pSVS (cloned SV40 WT830 [12]) with KpnI at nt 294, treatment of the DNA with T4 DNA polymerase, and ligation of the DNA in the presence of XhoI linker DNA (5'-dCCTCGAGG-3'). Plasmid pSV1771 is pSVS with a deletion of nt 502 through nt 528, inclusive (P. J. Good, Ph.D. thesis, University of Wisconsin, Madison, 1987). Plasmids pSV1777 and pSV1778 were constructed, respectively, by substitution of the HindIII (nt 1046)-to-StuI (nt 1461) and NcoI (nt 560)-to-StuI (nt 1461) fragments of pSVS with SalI linker DNA (5'-dGGTCGACC-3'). Plasmid pSD36 was constructed by insertion of the HpaII (nt 346)-to-HindIII (nt 1046) fragment of SV40 DNA into pUC18 DNA cut with AccI and HindIII. Plasmid pSV1773, lacking nt 1629 through nt 1635, inclusive, was constructed by partial digestion of pSVS with AccI, treatment of full-length linear DNA with S1 nuclease, and ligation to form monomer circles. Plasmid pSV1774 was constructed by insertion of SalI linker DNA into the StuI site at nt 1236 of pSVS.

Plasmid pSD5 (Fig. 2) was constructed by insertion of a poly(A) tract from the γ-globin cDNA plasmid p3'γ7 (a gift from K. Lang [34]) between the BamHI and HindIII sites of pSP65 (37) followed by insertion of BglII linker DNA (5'-dCAGATCTG-3') directly after the poly(A) tract. Plasmid pSD9-273 (Fig. 2) was constructed by insertion of a PvuII (nt 273)-to-HpaI (nt 2668) fragment of SV40 DNA into EcoRI (made blunt with S1 nuclease)–SmaI-cut pSD5, along with insertion of SalI linker DNA adjacent to the SP6 promoter. Plasmids containing cDNA copies of each of the late 19S

TABLE 1. Summary of late 19S RNA species present and rates of synthesis of VP2 relative to VP3
in cells infected with leader region mutants

Mutant	Nucleotides deleted[a]	19S RNA species (relative amt)[b]	Relative rate of synthesis of VP2 to VP3[c]
WT800		C (30–40%), D (50–60%), E (5%), F (<1%)	1
WT830		C (30–40%), D (50–60%), E (5%), F (<1%)	1
802	344–423	C (90%), Z (10%)	1.1 ± 0.1
805	331–517	C (90%), E (3%), Y (5%)	1.1 ± 0.1
806	222–359	ND	0.7 ± 0.1[d]
809	299–468	C (70%), E (5%), Y (20%)	1.2 ± 0.1
810-R3	297–471[e]	X (90%), E (8%)	1.4 ± 0.1
1770	294–298[f]	D (95%), E (5%)	2.0

[a] The SV40 nucleotide residues deleted, inclusive, were determined either previously (4; Somasekhar et al., in preparation) or for this report. WT800 and WT830 differ in the precise size of their duplicated enhancer region (54).

[b] The structures and relative abundances of the various cytoplasmic spliced 19S RNA species were determined from data presented in Fig. 3 and obtained previously (55; Barkan, Ph.D. thesis; data not shown); they were not determined (ND) for mutant 806. The letters C, D, E, and F refer to the RNA species depicted in Fig. 1. The letters X, Y, and Z refer to SV40 late 19S RNA species formed by the utilization of cryptic splice sites encoded within the mutant RNAs. For RNA species X, the first copy of a cryptic 5' splice site at nt 498 is joined to the 3' splice site at nt 558. For RNA species Y, the 5' splice site at 294 is joined to a cryptic 3' splice site at nt 536. The structure of RNA species Z has not been determined definitively. Each number in parentheses indicates the approximate percentage of SV40 cytoplasmic spliced late 19S RNAs having that structure. (The RNA species obtained from mutant 805 differ significantly from those reported previously [14, 16]; we do not understand the reason for these differences. P. K. Ghosh [personal communication] has confirmed this finding.)

[c] The rates of synthesis of VP2 relative to VP3 were determined as described in Materials and Methods and were normalized to the rate obtained with cells infected in parallel with WT virus. For all except mutant 1770, each is the mean and standard deviation from two separate infections, with each sample being immunoprecipitated at least three separate times. The absolute molar ratio for WT-infected cells was 0.4.

[d] 19S RNA species D from mutant 806 also encodes a fusion protein between VP2 and an ORF initiating with an AUG codon at nt 198 (Barkan, Ph.D. thesis).

[e] Mutant 810-R3 was isolated as a variant present in a serially passaged virus stock of mutant 810; in addition to the indicated deletion, the viral DNA contains a duplication of the leader region from nt 483 through nt 508, inclusive (Somasekhar et al., in preparation).

[f] Mutant 1770 also contains an 8-base-pair insertion of XhoI linker DNA (5'-dCCTCGAGG-3') at the site of the deletion.

RNA species are described elsewhere (18). The plasmids summarized in Table 2 were constructed by substitution of a PvuII (nt 273)-to-AccI (nt 1630) fragment of the respective cDNA plasmid in place of the SalI (filled in with the Klenow fragment of DNA polymerase I)-to-AccI fragment of pSD9-273.

Antisera. Antisera raised against gel-purified VP3 (gifts from H. Kasamatsu and S. Sedman) were used for the immunoprecipitation of VP2 and VP3 antiserum raised against whole virions (horse anti-SV40; Flow Laboratories, Inc.) was used for the immunoprecipitation of VP1. Antiserum raised in rabbits against gel-purified VP1 (a gift from S. Sedman) was used for detection of VP1 by immunoblotting. The anti-VP2-anti-VP3 serum used for immunoblotting was raised in rabbits against a gel-purified VP2-β-galactosidase fusion protein. The latter protein was made by insertion of the HaeII (nt 832)-to-StuI (nt 1463) fragment of SV40 DNA into the polylinker region of plasmid pHK412 (2, 58). After induction with 1 mM isopropyl-β-thiogalactopyranoside, the 130-kilodalton fusion protein was purified and injected into rabbits as described previously (17).

Analysis of virion proteins. At 40 h after infection (10 to 20 PFU per cell), monolayers of CV-1P cells were preincubated for 30 min with medium lacking the amino acid used for labeling and then pulse-labeled for the indicated times with the same medium supplemented with either [14C]arginine (10 μCi/ml, 330 Ci/mmol; Amersham Corp.) or [35S]methionine (100 μCi/ml, 1,200 Ci/mmol; Amersham). Whole-cell extracts were prepared as described either by Barkan et al. (6) or by Baichwal and Sugden (2). The proteins, either with or without prior immunoprecipitation with appropriate antisera, were resolved by electrophoresis in sodium dodecyl sulfate (SDS)–12% polyacrylamide (0.15% bisacrylamide) gels. The gels were impregnated with En³Hance (New England Nuclear Corp.), dried, and exposed to preflashed X-ray film (Eastman Kodak Co.). Immunoprecipitations were performed as described previously (25); lysates to be

immunoprecipitated with anti-VP2-3 serum were precleared by immunoprecipitation with anti-VP1 serum. The relative levels of VP2 and VP3 were determined by quantitative densitometry.

For the analysis of nonviable mutants, viral DNA was excised from the cloning vector, ligated into monomer circles, and transfected into CV-1PD cells as described by Good et al. (18). Proteins were harvested, electrophoresed in SDS–12% polyacrylamide gels, and then immunoblotted as described previously (2, 6).

In vitro transcription. BglII-linearized templates were transcribed as described by Krieg and Melton (33), except that [7meGpppG] (Pharmacia, Inc.) was included at 500 μM, the GTP concentration was lowered to 100 μM, and 2.5 μCi of [5,6-³H]UTP (35 Ci/mmol, ICN Pharmaceuticals, Inc.) was included to monitor polymerization. The yield of RNA was calculated by determining the percentage of [³H]UTP incorporated into material that bound to DE81 filters.

Full-length runoff transcripts were purified by a batch oligo(dT) procedure. RNA was suspended in 90 μl of 0.1% SDS in 10 mM Tris hydrochloride (pH 7.6)–1 mM EDTA (STE), incubated at 65°C for 5 min, cooled rapidly on ice, and made 0.5 M in LiCl. This RNA was mixed with 50 μl of packed volume of oligo(dT)-cellulose and incubated for 5 min at room temperature. After centrifugation in a microcentrifuge for 1 min, the resin was washed twice in STE containing 0.1 M LiCl. The bound poly(A)⁺ RNA was then eluted by three sequential incubations of the resin at 65°C in 100 μl of STE for 5 min, precipitated with ethanol, and suspended in water. The yield of poly(A)⁺ RNA ranged from 40 to 70% of the total ³H-labeled material.

Cell-free translation. Cell-free translation with a micrococcal nuclease-treated rabbit reticulocyte lysate was performed with a kit as directed by the supplier (Promega Biotec or Amersham). Poly(A)⁺ RNA was included as indicated in Fig. 5 and 6, and the proteins were labeled by incorporation of L-[4,5-³H]leucine (1 mCi/ml, 126 Ci/mmol;
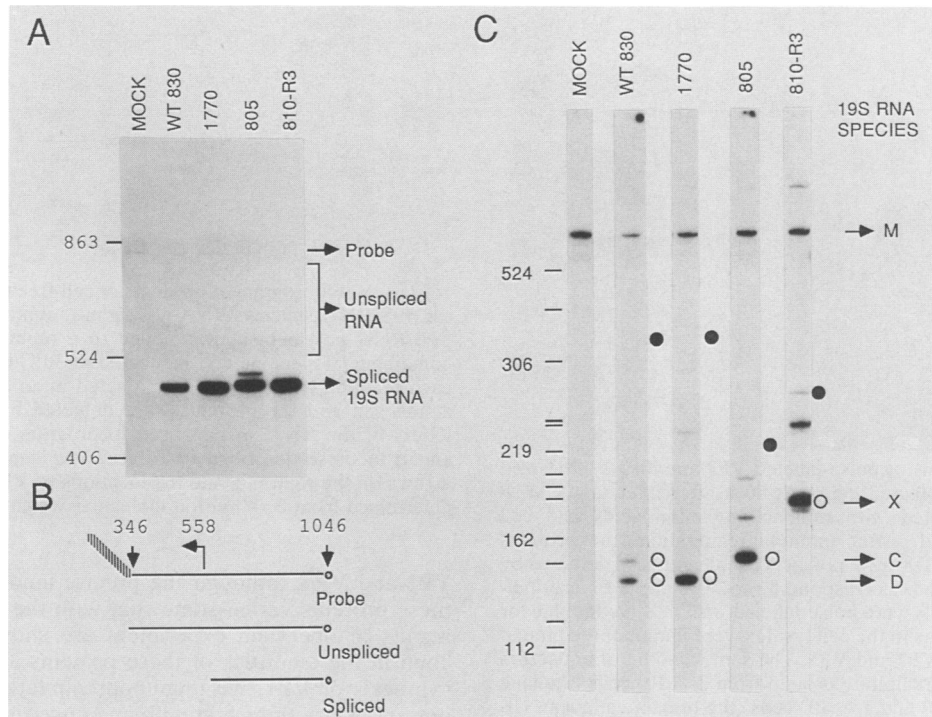
FIG. 3. Analysis of cytoplasmic 19S RNAs present in cells infected 40 h previously with WT830 and late leader region mutants. (A) Autoradiogram of S1 mapping analysis of the 19S RNAs. The levels of spliced and unspliced 19S RNA obtained from the cytoplasm of 10^4 infected cells were quantified by S1 mapping by using as probe a HindIII-to-BglI fragment of pSD36 5'-end-labeled at its HindIII site. The marks on the left indicate the positions of molecular weight markers, and the arrows on the right identify the locations of the probe and DNAs protected by either unspliced or spliced 19S RNA. The bands representing unspliced RNAs are heterogeneous in size owing to deletions present in the unspliced mutant RNAs. (B) Diagram of the predicted S1-resistant fragments from S1 mapping reactions with the pSD36 probe. The open circle and diagonal line represent the locations of the labeled 5' end and the vector sequences, respectively. (C) Autoradiogram of modified primer extension analysis of the 19S RNAs. The structures of the cytoplasmic RNAs obtained from 10^5 infected cells were determined by the modified primer extension assay (18). In brief, cDNAs were synthesized with a 19S-specific primer 5'-end-labeled at nt 682 and cleaved at nt 273 and nt 360 with PvuII and BstNI, respectively, after synthetic oligonucleotides which hybridize to the cDNAs at the locations of these restriction enzyme sites were annealed. The cDNAs were fractionated in a 5% polyacrylamide gel containing 8 M urea. The identities of the bands were determined from the expected sizes of the cleaved cDNAs. Symbols: O, locations of cleaved cDNAs made from spliced RNAs; ●, locations of cleaved cDNAs made from unspliced RNAs. RNA species C and D are as indicated in Fig. 1; RNA species X is a previously undetected spliced RNA which was formed by joining the first copy of a cryptic 5' splice site at nt 498 to the 3' splice site at nt 558; RNA species M indicates a cDNA made from cellular RNA. The marks on the left indicate the locations of MspI-cut pBR322 molecular weight markers.

New England Nuclear). Afterwards, the proteins were re-solved by electrophoresis in SDS–12% polyacrylamide gels. The levels of specific proteins were quantified by scintillation spectroscopy of excised protein bands solubilized with NCS (Amersham) as directed by the manufacturer.

RNA analysis. Cytoplasmic RNA was prepared by either of two methods (11, 49) and was treated with DNase I as described previously (18). The detailed procedures used for S1 mapping and modified primer extension analysis are described elsewhere (18). The probes for S1 mapping, derived from pSD36 and pSD52 (18) were hybridized to the RNAs at 52°C.

RESULTS

Rates of synthesis of VP2 relative to VP3 in cells infected with wild-type and mutant viruses that accumulate altered ratios of the 19S RNA species. To determine whether specific 19S RNA species are preferentially translated to synthesize only one of the virion proteins, we measured the rates of synthesis of VP2 relative to VP3 in cells infected with leader region mutants that accumulate the spliced 19S RNA species

in altered ratios. Each of the mutants listed in Table 1 has a deletion within its leader region which removes one or more of the splice sites used in the synthesis of some of the 19S RNA species. S1 mapping analysis of cytoplasmic viral RNAs obtained from cells infected with each of these mutants indicated that with the exception of mutant 809, more than 90% of the 19S RNAs were synthesized by using the normal 3' splice site at nt 558 (Fig. 3A; A. Barkan, Ph.D. thesis, University of Wisconsin, Madison, 1983). Analysis of these RNA samples by a modified primer extension technique indicated that at least 90% of the late 19S RNA found in cells infected with mutants 802, 805, 1770, and 810-R3 consisted of RNA species C, C, D, and a cryptically spliced 19S RNA species X, respectively (Fig. 3C; Table 1). In addition to differences in the ratios of the various spliced RNA species, the precise sequences of the leader regions of these RNAs differ because the deletions both remove specific sequences and shift upstream the locations of the 5' ends of the 19S RNAs (13, 14, 45, 55).

The rates of synthesis of VP2 relative to VP3 in cells infected in parallel with each of these mutants or with WT virus were determined by pulse-labeling the cells with either
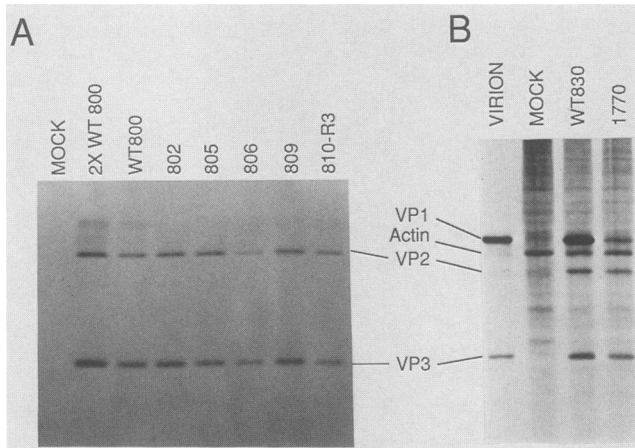
FIG. 4. Fluorograms of pulse-labeled VP2 and VP3 synthesized in WT- and mutant-infected cells. At 40 h after infection, CV-1P cells were pulse-labeled with radioactive amino acids and cell lysates were prepared. After immunoprecipitation, the proteins were fractionated in SDS–12% polyacrylamide gels and detected by fluorography. The bands corresponding to VP2 and VP3 are indicated. (A) Infected cells were pulse-labeled with [^{35}S]methionine for 20 min, and the proteins in the cell lysates were immunoprecipitated with an antiserum to VP2 and VP3. The same amount of antiserum was used to immunoprecipitate protein from 2×10^5 cells (the lane designated 2× WT800) and 1×10^5 cells (the remaining lanes). (B) The infected cells were pulse-labeled for 1 h with [^{14}C]arginine, and the proteins in the cell lysates were immunoprecipitated with antisera to both VP1 and VP2 and VP3. Lysate from 10^5 cells was used for each lane. The lane labeled VIRION contained [^{3}H]leucine-labeled virions.

[^{35}S]methionine or [^{14}C]arginine at 40 h after infection and resolving the virion proteins after immunoprecipitation by electrophoresis in SDS-polyacrylamide gels (Fig. 4). The results (Table 1) indicated that cells infected with each of these mutants synthesized VP2 and VP3 at similar relative rates, with small, reproducible differences from the WT ratio existing for some of the mutants (i.e., mutants 806, 810-R3, and 1770). Combining the RNA and protein data, we conclude that the various late 19S RNA species are not preferentially translated to produce either VP2 or VP3; however, the specific sequence of the leader region may influence somewhat the precise rate of synthesis of VP2 relative to VP3.

Cell-free translation of the individual 19S RNA species. To confirm that both VP2 and VP3 are synthesized efficiently from each of the spliced 19S RNA species, we analyzed proteins made in rabbit reticulocyte translation lysates programmed with individual 19S RNA species. To facilitate the purification of full-length poly(A)$^+$ RNA, we constructed the vector pSD5, which contains an SP6 promoter followed by a stretch of approximately 110 adenylic acid residues followed immediately thereafter by a unique BglII restriction enzyme site (Fig. 2). We have already isolated plasmids which correspond to cDNA copies of the SV40 late RNA species B through F (Fig. 1) (18). The late regions of these cDNA plasmids were inserted into pSD5 to generate the plasmids listed in Table 2.

Capped full-length poly(A)$^+$ RNAs corresponding in structure to each of the late 19S RNA species were synthesized (Fig. 2) and individually translated in a micrococcal nuclease-treated rabbit reticulocyte lysate in the presence of [^{3}H]leucine. Each of the translation reactions predominantly synthesized proteins that comigrated with the virion proteins

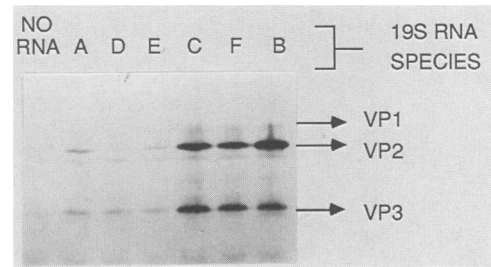FIG. 5. Fluorogram of products of cell-free translation of each of the 19S RNA species. RNA (10 µg/ml), synthesized in vitro with SP6 RNA polymerase, was added to a rabbit reticulocyte lysate containing [^{3}H]leucine and incubated at 30°C for 1 h. A portion of each reaction mixture was fractionated in an SDS–12% polyacrylamide gel, and the proteins were detected by fluorography. The letters of the RNA species used to program each reaction correspond to those described in Table 2 and depicted in Fig. 1. The arrows on the right indicate the locations of VP1, VP2, and VP3 as determined from SV40 virion molecular weight markers.

VP2 and VP3, although the precise amounts and ratios of these proteins varied somewhat with the RNA species (the results of one such experiment are shown in Fig. 5). To confirm the identities of these proteins and to look for the synthesis of VP1, we immunoprecipitated the products of one set of reactions first with an antiserum to VP1 (Fig. 6A) and then with an antiserum to VP2 and VP3 (Fig. 6B). These data show that lysates programmed with each RNA species did make some VP1, although at a low level (less than 10% of the level of VP2 plus VP3). Immunoprecipitation with an antiserum to VP2 and VP3 confirmed that the two major proteins were, indeed, VP2 and VP3 (Fig. 6B).

The amounts of VP2 and VP3 synthesized in the cell-free extracts programmed with the in vitro-synthesized 19S RNA species were quantified and are summarized in Table 2. The most striking observation is that RNAs lacking an AUG codon upstream of the VP2 AUG codon yielded three- to
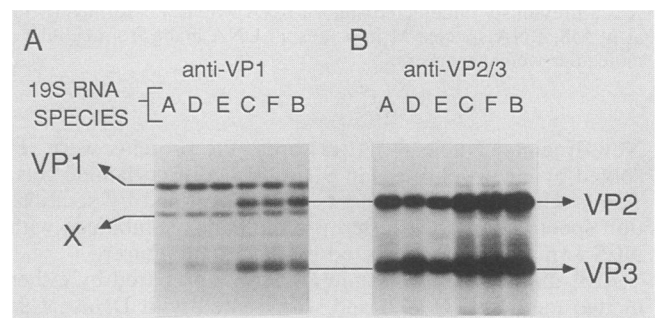

FIG. 6. Fluorogram of virion proteins immunoprecipitated from cell-free translation reactions of each of the 19S RNA species. Translation products synthesized as described in the legend to Fig. 5 were immunoprecipitated first with an antiserum to VP1 (A); the resulting supernatant was then immunoprecipitated with an antiserum to VP2 and VP3 (B). Both sets of immunoprecipitates were fractionated in an SDS–12% polyacrylamide gel. The lanes are labeled as described in the legend to Fig. 5. The protein labeled X is a VP1-immunoreactive protein of unknown origin. VP2 and VP3 contaminated the VP1 immunoprecipitates because of the large molar excess of VP2 and VP3 in the reaction mixtures, combined with a tendency of VP1 to aggregate with VP2 and VP3 (Barkan, Ph.D. thesis). Panels A and B were made from X-ray films exposed for the same length of time so that the amounts of VP1 can be compared directly with the amounts of VP2 and VP3; the fluorogram shown here is outside the linear range of the film for VP2 and VP3.

TABLE 2. Summary of the plasmids used and the data obtained from the cell-free synthesis and translation
of each of the late 19S RNA species

Plasmid	19S RNA species[a]	Sequences deleted[b]	LP1 AUG codon[c]	Molar ratio (VP2 to VP3)[d]	Relative rate of synthesis of VP2 + VP3[e]
pSD9-273[f]	A		+	0.5 ± 0.1	1
pSD-B	B	295–434	−	1.4 ± 0.6	5.2 ± 1.8
pSD-C	C	295–557	−	0.6 ± 0.1	3.9 ± 1.6
pSD-D	D	374–557	+	0.3 ± 0.1	1.0 ± 0.3
pSD-E	E	527–557	+	0.5 ± 0.1	1.1 ± 0.5
pSD-F	F	294–434, 527–557	−	0.6 ± 0.1	3.1 ± 1.3

[a] The letters refer to the RNA species depicted in Fig. 1.

[b] Each deletion corresponds precisely to a known intervening sequence.

[c] + and −, Presence and absence, respectively, of the LP1 AUG codon at nt 335.

[d] Molar ratios of VP2 to VP3 synthesized in cell extracts programmed with the indicated RNA species. These ratios were determined by quantification of radioactivity in bands of VP2 and VP3 excised from gels similar to the one shown in Fig. 5, calculation of the molar dpm per protein by division of the dpm in VP2 and VP3 by the number of leucine residues in the proteins (i.e., 29 and 19, respectively), and then division of the molar dpm in VP2 by the molar dpm in VP3. The numbers represent means and standard deviations from three experiments.

[e] The relative amounts of VP2 plus VP3 synthesized in cell extracts programmed with the RNA species indicated. For each experiment, these amounts were determined by adding the molar dpm in VP2 and VP3 for each reaction and dividing by the value obtained for RNA species A. The numbers represent means and standard deviations from three experiments.

[f] The exact structure of this plasmid is diagrammed in Fig. 2; the others are derivatives of it constructed as described in Materials and Methods.

fivefold more VP2 plus VP3 than did RNAs containing an upstream AUG codon. Assuming a leucine concentration of 10 μM in the rabbit reticulocyte lysate (23), we calculated for one of the experiments a molar ratio of synthesized protein to input RNA ranging from 8 to 56. In addition, the ratio of VP2 to VP3 varied somewhat with the particular RNA species translated. In summary, we conclude definitively that each of the 19S RNA species functionally encodes both VP2 and VP3; however, the precise sequence of the leader region of the 19S RNA species affects somewhat the precise relative and absolute levels of synthesis of these proteins.

Lack of synthesis of VP1 from the 19S RNAs in monkey cells. A small amount of VP1 was synthesized during cell-free translation of the 19S RNA species. To determine whether VP1 was synthesized from 19S RNA species in SV40 DNA-transfected monkey cells, we used a mutant, SV1771, that lacks nt 502 through nt 528, inclusive, which encode the 5' splice site normally used in the synthesis of the late 16S RNAs. Genetic analysis showed that this mutant complemented D- but not B-group mutants (data not shown), implying a defect in VP1 synthesis. CV-1PD cells transfected with viral DNA of mutant SV1771 accumulated 16S RNAs to levels less than 2% the amount found in cells transfected in parallel with WT DNA (Fig. 7B). The same cells accumulated VP1 to levels less than 1% of the amount found in cells transfected in parallel with WT DNA (Fig. 7A), yet accumulated 19S RNAs (Fig. 7B) and VP3 (data not shown) to normal levels. Thus, the late 19S RNA species do not function as templates for VP1 synthesis in monkey cells.

The absence of VP1 synthesis from the 19S RNAs may be due to the presence of numerous translation initiation signals which, taken together, prevent scanning ribosomes from reaching the VP1 initiation signal. To test this hypothesis, we constructed mutants SV1777 and SV1778, which lack both the 3' splice site used to synthesize the 16S RNAs and some of the AUG codons situated between the 5' end of the 19S RNAs and the VP1 initiation codon. As expected, cells transfected with SV1777 and SV1778 accumulated only 19S-like RNAs (Fig. 7B; data not shown); however, they accumulated, respectively, approximately 0.03 and 0.15 of the amount of VP1 from these RNAs as SVS-transfected cells did from 16S RNA (Fig. 7). Thus, we conclude that VP1 can be synthesized from the 19S RNAs in monkey cells when the number of translation initiation signals situated

upstream of the VP1 ORF is decreased, with the amount of VP1 synthesized being inversely related to their number.

DISCUSSION

Synthesis of both VP2 and VP3 from each of the 19S RNA species. The experiments presented above were designed to determine whether certain of the late 19S RNA species of SV40 are translated to produce preferentially either VP2 or VP3. Analysis of the virion proteins and the structures of the 19S RNAs made in cells infected with viable leader region mutants indicated that although the ratios of the 19S RNA species differed from those found in WT-infected cells, the rates of synthesis of VP2 relative to VP3 were similar for all (Fig. 3 and 4; Table 1). Furthermore, translation in a rabbit reticulocyte lysate resulted in the synthesis of both VP2 and VP3 from each of the individual RNA species tested (Fig. 5; Table 2). Therefore, both VP2 and VP3 are synthesized from each of the late 19S RNA species of SV40, with no mechanism existing for a significant preferential translation of one virion protein from any one of these RNA species.

Cell-free translation of individual 19S RNA species. Our data derived from cell-free translation of the individual 19S RNA species are consistent with previously published reports (8, 21, 46, 50). These reports showed that cell-free translation of SV40 late RNAs which are 19S in size results in the synthesis of all three of the virion proteins, with small variations in the VP2-to-VP3 ratio being observed with translation of the different size classes of the 19S RNAs. These small variations are similar to those noted here in the ratio of VP2 to VP3 synthesized from the individual 19S RNA species. We believe that the synthesis of VP1 and proteins related to VP1 (Fig. 6 [21]) is an artifact of using cell-free translation extracts and results from translation of partially degraded RNAs in which many of the AUG codons situated upstream of the VP1 initiation signal have been lost from the RNA (43). Both our finding that VP1 synthesis was readily observed when the translations were performed with saturating concentrations of 19S RNA (data not shown) and the data of others (8) support this hypothesis. However, the alternative possibilities that ribosomes (i) initiate translation at a low efficiency internally without scanning (19, 20, 52) or (ii) have a more relaxed scanning mechanism in the cell extract (40) have not been ruled out.
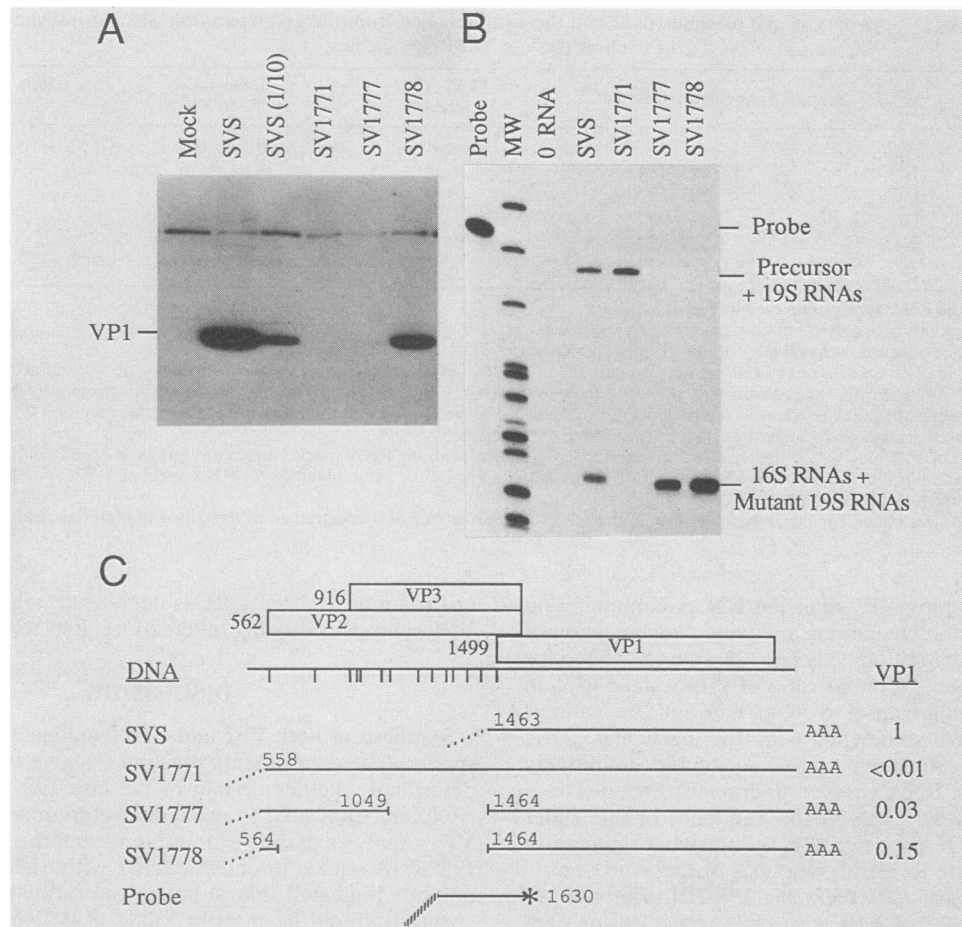
FIG. 7. VP1 synthesis in cells transfected with mutants that synthesize only 19S RNAs. (A) Autoradiogram of immunoblot of VP1 present in cells transfected with SVS and mutants SV1771, SV1777, and SV1778. CV-1PD cells were transfected with viral DNA excised from the plasmids indicated. At 44 h later, protein lysates were prepared. Proteins from lysates corresponding to 10^5 cells were separated in an SDS–12% polyacrylamide gel and transferred electrophoretically to nitrocellulose. The filter was probed first with a polyclonal antiserum to VP1 and then with ^{125}I-protein A (Amersham). The lane labeled SVS(1/10) contained lysate from 1×10^4 cells transfected with SVS diluted with lysate from 9×10^4 mock-transfected cells. The location of VP1 is indicated. (B) Autoradiogram of S1 mapping analysis of whole-cell RNAs. Whole-cell RNAs isolated from 5×10^4 cells were analyzed by S1 mapping with an AccI (nt 1630)-cut, 5'-end-labeled probe made from pSD52. The resulting S1 nuclease-resistant fragments were electrophoresed in a 5% polyacrylamide gel containing 8 M urea. The lanes labeled Probe, MW, and 0 RNA contained 1/25th the amount of probe used in each reaction, MspI-cut pBR322 molecular weight markers, and an S1 reaction without added RNA, respectively. The bands are identified by the RNA species which they represent. (C) Structures of the RNAs and relative amounts of VP1 accumulated in cells transfected with mutants that synthesize only 19S RNAs. The boxes at the top indicate the ORFs for the respective proteins, with the numbers denoting the first nucleotide of each ORF. The marks on the line underneath the boxes indicate the locations of AUG codons between the VP2 and the VP1 initiation codons. The next four lines depict the structures of the late viral RNAs from which VP1 was synthesized in the transfected cells. The dotted lines and blank spaces indicate the locations of excised introns and sequences deleted in the mutants, respectively. The numbers indicate the locations of the endpoints of novel joints resulting from splicing and the deletion mutations. The RNAs from mutants SV1777 and SV1778 contain the sequence 5'-GGTCGACC-3' from linker DNA at the site of the deletions. The relative amounts of accumulated VP1 were determined from densitometric analysis of autoradiograms similar to those shown in panels A and B, with normalization of the relative amounts of VP1 to the relative amounts of 19S-like RNAs (i.e., RNAs synthesized by splicing at nt 558) or, for SVS-transfected cells, 16S RNAs. The bottom line indicates the structure of the pSD52 probe used for S1 mapping; the asterisk and the diagonal line indicate the labeled 5' end and non-SV40 sequences, respectively.

Decrease in the efficiency of translation of downstream ORFs by upstream AUGs. Cell-free translations of the late 19S RNA species that retain the LP1 AUG codon at nt 335 synthesized both VP2 and VP3 three- to fivefold less efficiently than did RNA species that lack it (Table 2). Thus, the LP1 AUG codon significantly, although not completely, suppresses translation of downstream ORFs (i.e., VP2 and VP3). This interference indicates that ribosomes initiate translation efficiently at the LP1 AUG, a not unexpected conclusion given that the sequences surrounding the LP1 initiator codon define a strong initiation signal (32). Evidence

in support of these conclusions includes the following. (i) The 16S RNA species that contains the LP1 initiation codon is found, on average, on smaller polysomes than are 16S RNA species that lack this signal (5). (ii) Cells infected with WT SV40 synthesize LP1 and VP1 at similar rates (C. Hussussian, S. A. Sedman, and J. E. Mertz, unpublished data). (iii) Cells transfected with mutants that encode fusion proteins between the LP1 and VP2 ORFs and the LP1 and VP1 ORFs synthesize these fusion proteins at rates similar to those for the unfused proteins (data not shown; S. A. Sedman and J. E. Mertz, unpublished data). Therefore, in

the presence of a translatable ORF within the leader region, translation of the downstream VP2 and VP3 ORFs is a function of (i) the efficiency of scanning past the LP1 initiation signal and (ii) the efficiency of reinitiation following termination of translation of the LP1 ORF.

We have not quantified the effect of the LP1 AUG codon on the translation of ORFs situated downstream from it in infected monkey cell because the mutations that we examined result in upstream shifts in the locations of the 5' ends of most of the 19S RNAs such that they might encode additional upstream AUG codons and ORFs within their leader regions. However, other workers have noted a decrease in the efficiency of translation of downstream ORFs as a result of the presence of the LP1 initiation signal in monkey cells transfected with (i) SV40 mutants, differing only in the presence of the LP1 initiation codon, that synthesize predominantly one spliced late RNA species (Sedman and Mertz, unpublished data) and (ii) SV40 late region replacement vectors which either contain or lack the LP1 initiation codon (44). In addition, suppression of translation of downstream ORFs by upstream AUG codons has been observed in the translation of the other naturally occurring (26) and synthetic (3, 29, 59) mRNAs. Therefore, our conclusion that the presence of the LP1 initiation codon decreases the efficiency of translation of downstream ORFs appears to be true for both cell-free translation extracts and infected monkey cells.

Differences in the rates of synthesis of VP2 to VP3. Although cell-free translations of each of the 19S RNA species resulted in the synthesis of both VP2 and VP3, the ratio of VP2 to VP3 synthesis was significantly lower from 19S RNA species D than from the other 19S RNA species (Table 2). We hypothesize that this finding results from efficient translation of a 90-nt ORF encoded within RNA species D beginning at the LP1 initiation codon and terminating at a termination codon situated 48 nt downstream of the VP2 initiation codon (39, 45, 48). The lower amount of VP2 relative to VP3 synthesized from this RNA species could be due to ribosomes that translate this ORF (i) interfering somewhat with translation initiation at the VP2 initiation codon and (ii) reinitiating translation preferentially at the VP3 initiation codon following termination downstream of the VP2 initiation codon. The 30-amino-acid polypeptide encoded by the spliced 19S RNA species D has not been directly identified. However, cells transfected with an appropriate late leader region frameshift mutant synthesize efficiently from 19S RNA species D the predicted LP1-VP2 fusion protein (Sedman and Mertz, unpublished data). Therefore, this ORF is probably translated efficiently, with its translation influencing differentially the efficiencies of translation initiation at the VP2 and VP3 ORFs.

The data obtained with mutant-infected monkey cells for the relative ratio of VP2 to VP3 synthesized from a particular 19S RNA species differed somewhat from those obtained with the cell-free translation system. For example, although cell-free translation of 19S RNA species D resulted in twofold-lower synthesis of VP2 relative to VP3 than did cell-free translation of 19S RNA species C (Table 2), cells infected with mutant 1770, which produced predominantly 19S RNA species D, synthesized twofold more VP2 relative to VP3 than did cells infected with mutants that produced predominantly 19S RNA species C (e.g., mutant 805; Table 1). However, the 19S RNAs synthesized in monkey cells infected with these leader region mutants are heterogeneous, differing not only in the introns they lack, but also in the precise sequences of their leader regions because of alter-

ations in both the sequences of the leader regions of the mutants and the locations of the 5' ends of the predominant RNA species made from them (14, 16; data not shown). Therefore, we do not know how to interpret the differences in the rate of synthesis of VP2 relative to VP3 observed in leader region mutant-infected monkey cells except to say that the sequence of the leader region can affect the rates of synthesis of VP2 and VP3. A similar variation in the efficiency of translation of retrovirus RNAs with different leader regions has been noted (24).

On the other hand, the data summarized in Table 2 concerning differences in the VP2-to-VP3 ratios are interpretable because they were obtained with homogeneous populations of defined RNAs. In addition, the finding of Sedman and Mertz (unpublished data) that the rate of synthesis of VP2 relative to VP3 is lower in cells transfected with mutant 1770 than it is in cells transfected with mutant 1770 containing a point mutation at the LP1 initiation codon indicates that translation of the leader region influences the efficiencies of translation of the VP2 and VP3 ORFs in monkey cells in the same manner as it does in cell extracts.

VP1 synthesis from 19S RNAs. Cells transfected with the mutant SV1771, containing 19S but not 16S RNAs, accumulated less than 1% of the level of VP1 found in WT-transfected cells (Fig. 7). Therefore, VP1 is not translated from the 19S RNAs in monkey cells. However, Berg and co-workers (42, 56) concluded that the ORF encoding dihydrofolate reductase is translated efficiently on an SV40 late 19S-like RNA molecule when inserted after the VP3 initiation codon. The difference between our result with mutant SV1771 and theirs stems from the sequences situated between the VP3 initiation codon and the downstream, assayed ORF. Although the 19S-like RNAs described by Berg and co-workers (42, 56) contain 3 AUGs in the 130 nt of sequence between the VP3 initiation codon and the dihydrofolate reductase initiation codon, the 19S RNAs of SV40 contain 10 AUGs in the 583 nt of sequence between the VP3 initiation codon and the VP1 AUG codon (10). If one assumes that ribosomes scan the RNA from the 5' end before initiation, some ribosomes would appear to be able to scan past the VP2 and VP3 initiation codons; however, few, if any, are able to scan on WT 19S RNA all the way to the VP1 initiation codon because of the presence of the numerous additional AUG codons. Consistent with this explanation, VP1 was synthesized from the late 19S RNAs made in cells transfected with mutants containing either large deletions upstream of the VP1 initiation codon (Fig. 7) or a point mutation at the VP3 initiation codon (data not shown), with the amount of the VP1 synthesized being inversely proportional to the number of AUG codons situated upstream of the VP1 initiation signal. Our finding that cells transfected with mutant 1778 still make 5- to 10-fold less VP1 than do cells transfected with WT SV40 is probably due to the late 19S RNAs made from the mutant differing from those of WT 16S RNAs by having LP1- and VP2-initiated ORFs which terminate downstream of the VP1 initiation signal.

Model for the regulation of VP2 and VP3 synthesis. What determines the rates of synthesis of VP2 and VP3 from a single SV40 late 19S RNA species? We have shown that the sequences in the leader region do not dramatically affect the rate of synthesis of VP2 relative to VP3. Other workers (41, 51) have demonstrated that proteins encoded by the 19S RNAs of SV40 are synthesized via a mechanism consistent with a leaky scanning model of translation initiation (27). Therefore, we hypothesize that the rates of synthesis of VP2 and VP3 are determined largely by the relative efficiency

with which ribosomes initiate translation at the VP2 initiation codon; ribosomes which fail to initiate or reinitiate there scan past it and initiate translation at the VP3 initiation codon instead. The sequence requirements for a strong initiation signal have been identified by the examination of eucaryotic initiation codons (27, 28) and confirmed by mutational analysis (30). On the basis of these data, the VP2 initiation signal is weak, whereas the VP3 initiation signal is strong (32). This hypothesis explains why (i) the rate of synthesis of VP3 is greater than that of VP2 (Tables 1 and 2) and (ii) cells transfected with a mutant that lacks the VP2 initiation codon accumulate more VP3 than do cells transfected with WT (51).

Translation of the late RNAs of SV40. In summary, we conclude from the results presented here that each of the 19S RNA species is translated to yield both VP2 and VP3, whereas each of the 16S RNA species is translated to yield VP1. The 61-amino-acid protein LP1 is synthesized from 19S RNA species E and 16S RNA species G, although mostly from the latter because of its much greater abundance. Lastly, the rates of synthesis of VP2 and VP3 are determined largely by the efficiency with which ribosomes initiate translation at the VP2 initiation codon. The factors affecting translation initiation at the VP2 initiation codon are (i) the strength of the initiation signal and (ii) the arrangement, when present, of upstream ORFs within the leader region.

LITERATURE CITED

1. **Aloni, Y., and N. Hay.** 1985. Attenuation may regulate gene expression in animal viruses and cells. Crit. Rev. Biochem. **18:**327–383.
2. **Baichwal, V. R., and B. Sugden.** 1987. Posttranslational processing of an Epstein-Barr virus-encoded membrane protein expressed in cells transformed by Epstein-Barr virus. J. Virol. **61:**866–875.
3. **Bandyopadhyay, P. K., and H. M. Temin.** 1984. Expression from an internal AUG codon of herpes simplex thymidine kinase gene inserted in a retrovirus vector. Mol. Cell. Biol. **4:**743–748.
4. **Barkan, A., and J. E. Mertz.** 1981. DNA sequence analysis of simian virus 40 mutants with deletions mapping in the leader region of the late viral mRNA's: mutants with deletions similar in size and position exhibit varied phenotypes. J. Virol. **37:**730–737.
5. **Barkan, A., and J. E. Mertz.** 1984. The number of ribosomes on simian virus 40 late 16S mRNA is determined in part by the nucleotide sequence of its leader. Mol. Cell. Biol. **4:**813–816.
6. **Barkan, A., R. C. Welch, and J. E. Mertz.** 1987. Missense mutations in the VP1 gene of simian virus 40 that compensate for defects caused by deletions in the viral agnogene. J. Virol. **61:**3190–3198.
7. **Celma, M. L., R. Dhar, J. Pan, and S. M. Weissman.** 1977. Comparison of the nucleotide sequence of the messenger RNA for the major structural protein of SV40 with the DNA sequence encoding the amino acids of the protein. Nucleic Acids Res. **4:**2549–2559.
8. **Cepko, C. L., U. Hansen, H. Handa, and P. A. Sharp.** 1981. Sequential transcription-translation of simian virus 40 by using mammalian cell extracts. Mol. Cell. Biol. **1:**919–931.
9. **Cole, C. N., T. Landers, S. P. Goff, S. Manteuil-Brutlag, and P. Berg.** 1977. Physical and genetic characterization of deletion mutants of simian virus 40 constructed in vitro. J. Virol. **24:**277–294.
10. **Contreras, R., R. Rogiers, A. Van de Voorde, and W. Fiers.** 1977. Overlapping of the VP2-VP3 gene and the VP1 gene in the SV40 genome. Cell **12:**529–538.
11. **Favaloro, J., R. Treisman, and R. Kamen.** 1980. Transcription maps of polyoma virus-specific RNA: analysis by two-dimensional nuclease S1 gel mapping. Methods Enzymol. **65:**718–749.
12. **Fromm, M., and P. Berg.** 1982. Deletion mapping of DNA regions required for SV40 early region promoter function in vivo. J. Mol. Appl. Genet. **1:**457–481.
13. **Gheysen, D., A. Van de Voorde, R. Contreras, J. Vanderheyden, F. Duerinck, and W. Fiers.** 1983. Simian virus 40 mutants carrying extensive deletions in the 72-base-pair repeat region. J. Virol. **47:**1–14.
14. **Ghosh, P. K., M. Piatak, J. E. Mertz, S. M. Weissman, and P. Lebowitz.** 1982. Altered utilization of splice sites and 5' termini in late RNAs produced by leader region mutants of simian virus 40. J. Virol. **44:**610–624.
15. **Ghosh, P. K., V. B. Reddy, J. Swinscoe, P. Lebowitz, and S. M. Weissman.** 1978. Heterogeneity and 5'-terminal structures of the late RNAs of simian virus 40. J. Mol. Biol. **126:**813–846.
16. **Ghosh, P. K., P. Roy, A. Barkan, J. E. Mertz, S. M. Weissman, and P. Lebowitz.** 1981. Unspliced functional late 19S mRNAs containing intervening sequences are produced by a late leader mutant of simian virus 40. Proc. Natl. Acad. Sci. USA **78:**1386–1390.
17. **Gilmore, T. D., and H. M. Temin.** 1986. Different localization of the product of the v-rel oncogene in chicken fibroblasts and spleen cells correlates with transformation by REV-T. Cell **44:**791–800.
18. **Good, P. J., R. C. Welch, W.-S. Ryu, and J. E. Mertz.** 1988. The late spliced 19S and 16S RNAs of simian virus 40 can be synthesized from a common pool of transcripts. J. Virol. **62:**563–571.
19. **Hassin, D., R. Korn, and M. S. Horwitz.** 1986. A major internal initiation site for the in vitro translation of the adenovirus DNA polymerase. Virology **155:**214–224.
20. **Herman, R. C.** 1986. Internal initiation of translation on the vesicular stomatitis virus phosphoprotein mRNA yields a second protein. J. Virol. **58:**797–804.
21. **Hunter, T.** 1979. Functional characterization of the early and late mRNAs of simian virus 40. Virology **95:**511–522.
22. **Hunter, T., and W. Gibson.** 1978. Characterization of the mRNA's for the polyoma virus capsid proteins VP1, VP2, and VP3. J. Virol. **28:**240–253.
23. **Jackson, R. J., and T. Hunt.** 1983. Preparation and use of nuclease-treated rabbit reticulocyte lysates for the translation of eukaryotic messenger RNA. Methods Enzymol. **96:**50–74.
24. **Katz, R. A., B. R. Cullen, R. Malavarca, and A. M. Skalka.** 1986. Role of avian retrovirus mRNA leader in expression: evidence for novel translational control. Mol. Cell. Biol. **6:**372–379.
25. **Kessler, S. W.** 1975. Rapid isolation of antigens from cells with a staphylococcal protein A-antibody adsorbent: parameters of the interaction of antibody-antigen complexes with protein A. Immunology **115:**1617–1624.
26. **Khalili, K., J. Brady, and G. Khoury.** 1987. Translational regulation of SV40 early mRNA defines a new viral protein. Cell **48:**639–645.
27. **Kozak, M.** 1981. Possible role of flanking nucleotides in recognition of the AUG initiator codon by eukaryotic ribosomes. Nucleic Acids Res. **9:**5233–5252.
28. **Kozak, M.** 1984. Compilation and analysis of sequences upstream from the translational start site in eukaryotic mRNAs.

Nucleic Acids Res. 12:857–872.

29. Kozak, M. 1984. Selection of initiation sites by eucaryotic ribosomes: effect of inserting AUG triplets upstream from the coding sequence for preproinsulin. Nucleic Acids Res. 12:3873–3892.

30. Kozak, M. 1986. Point mutations define a sequence flanking the AUG initiator codon that modulates translation by eukaryotic ribosomes. Cell 44:283–292.

31. Kozak, M. 1986. Influences of mRNA secondary structure on initiation by eukaryotic ribosomes. Proc. Natl. Acad. Sci. USA 83:2850–2854.

32. Kozak, M. 1986. Regulation of protein synthesis in virus-infected animal cells. Adv. Virus Res. 31:229–292.

33. Krieg, P. A., and D. A. Melton. 1984. Functional messenger RNAs are produced by SP6 in vitro transcription of cloned cDNAs. Nucleic Acids Res. 12:7057–7070.

34. Lang, K. M., and R. A. Spritz. 1985. Cloning specific complete polyadenylylated 3'-terminal cDNA segments. Gene 33:191–196.

35. Lebowitz, P., and S. M. Weissman. 1979. Organization and transcription of the simian virus 40 genome. Curr. Top. Microbiol. Immunol. 87:43–172.

36. Maniatis, T., E. F. Fritsch, and J. Sambrook. 1982. Molecular cloning: a laboratory manual. Cold Spring Harbor Laboratory, Cold Spring Harbor, N.Y.

37. Melton, D. A., P. A. Krieg, M. R. Rebagliati, T. Maniatis, K. Zinn, and M. R. Green. 1984. Efficient in vitro synthesis of biologically active RNA and RNA hybridization probes from plasmids containing a bacteriophage SP6 promoter. Nucleic Acids Res. 12:7035–7056.

38. Mertz, J. E., and P. Berg. 1974. Defective simian virus 40 genomes: isolation and growth of individual clones. Virology 62:112–124.

39. Nomura, S., G. Jay, and G. Khoury. 1986. Spontaneous deletion mutants resulting from a frameshift insertion in the simian virus 40 agnogene. J. Virol. 58:165–172.

40. Parker, P. J., L. Coussens, N. Totty, L. Rhee, S. Young, E. Chen, S. Stabel, M. D. Waterfield, and A. Ullrich. 1986. The complete primary structure of protein kinase C—the major phorbol ester receptor. Science 233:853–859.

41. Peabody, D. S., and P. Berg. 1986. Termination-reinitiation occurs in the translation of mammalian cell mRNAs. Mol. Cell. Biol. 6:2695–2703.

42. Peabody, D. S., S. Subramani, and P. Berg. 1986. Effect of upstream reading frames on translation efficiency in simian virus 40 recombinants. Mol. Cell. Biol. 6:2704–2711.

43. Pelham, H. R. B. 1979. Translation of fragmented viral RNA in vitro: initiation at multiple sites. FEBS Lett. 100:195–199.

44. Perez, L., J. W. Wills, and E. Hunter. 1987. Expression of the Rous sarcoma virus env gene from a simian virus 40 late-region replacement vector: effects of upstream initiation codons. J. Virol. 61:1276–1281.

45. Piatak, M., K. N. Subramanian, P. Roy, and S. M. Weissman. 1981. Late messenger RNA production by viable simian virus 40 mutants with deletions in the leader region. J. Mol. Biol. 153:589–618.

46. Prives, C. L., and H. Shure. 1979. Cell-free translation of simian virus 40 16S and 19S L-strand-specific mRNA classes to simian virus 40 major VP-1 and minor VP-2 and VP-3 capsid proteins. J. Virol. 29:1204–1212.

47. Reddy, V. B., P. K. Ghosh, P. Lebowitz, and S. M. Weissman. 1978. Gaps and duplicated sequences in the leaders of SV40 16S RNA. Nucleic Acids Res. 5:4195–4213.

48. Resnick, J., and T. Shenk. 1986. Simian virus 40 agnoprotein facilitates normal nuclear location of the major capsid polypeptide and cell-to-cell spread of virus. J. Virol. 60:1098–1106.

49. Ross, J. 1976. A precursor of globin messenger RNA. J. Mol. Biol. 106:403–420.

50. Rozenblatt, S., R. C. Mulligan, M. Gorecki, B. E. Roberts, and A. Rich. 1976. Direct biochemical mapping of eukaryotic viral DNA by means of a linked transcription-translation cell-free system. Proc. Natl. Acad. Sci. USA 73:2747–2751.

51. Sedman, S. A., and J. E. Mertz. 1988. Mechanisms of synthesis of virion proteins from the functionally bigenic late mRNAs of simian virus 40. J. Virol. 62:954–961.

52. Shih, D. S., I.-W. Park, C. L. Evans, J. M. Jaynes, and A. C. Palmenberg. 1987. Effects of cDNA hybridization on translation of encephalomyocarditis virus RNA. J. Virol. 61:2033–2037.

53. Siddell, S. G., and A. E. Smith. 1978. Polyoma virus has three late mRNA's: one for each virion protein. J. Virol. 27:427–431.

54. Somasekhar, M. B., and J. E. Mertz. 1985. Sequences involved in determining the locations of the 5' ends of the late RNAs of simian virus 40. J. Virol. 56:1002–1013.

55. Somasekhar, M. B., and J. E. Mertz. 1985. Exon mutations that affect the choice of splice sites used in processing the SV40 late transcripts. Nucleic Acids Res. 13:5591–5609.

56. Subramani, S., R. Mulligan, and P. Berg. 1981. Expression of the mouse dihydrofolate reductase complementary deoxyribonucleic acid in simian virus 40 vectors. Mol. Cell. Biol. 1:854–864.

57. Tooze, J. (ed.). 1981. DNA tumor viruses. The molecular biology of tumor viruses, part 2, 2nd ed., rev. Cold Spring Harbor Laboratory, Cold Spring Harbor, N.Y.

58. Watson, R. J., J. H. Weis, J. S. Salstrom, and L. W. Enquist. 1984. Bacterial synthesis of herpes simplex virus types 1 and 2 glycoprotein D antigens. J. Invest. Dermatol. 83:102s–111s.

59. Zitomer, R. S., D. A. Walthall, B. C. Rymond, and C. P. Hollenberg. 1984. Saccharomyces cerevisiae ribosomes recognize non-AUG initiation codons. Mol. Cell. Biol. 4:1191–1197.